Thermal quasiparticle correlations and continuum coupling in nuclei far from stability

N. Dinh Dang[1,2] and A. Arima[3]
[1]*RI-beam factory project office, RIKEN, 2-1 Hirosawa, Wako, 351-0198 Saitama, Japan*
[2]*Institute for Nuclear Science and Technique, VAEC, Hanoi, Vietnam*
[3]*House of Councilors, 2-1-1 Nagata-cho, Chiyoda-ku, Tokyo 100-8962, Japan*
(Received 9 April 2002; revised manuscript received 5 November 2002; published 16 January 2003)

The contributions of quasiparticle correlations and of continuum coupling upon the superfluid properties of neutron-rich Ni isotopes are studied within the modified BCS (MBCS) approximation at finite temperature. The effect of quasiparticle correlations is included using a secondary Bogoliubov-type canonical transformation explicitly involving the quasiparticle occupation numbers at temperature T. The effect of continuum coupling is taken into account via the finite widths of the resonant states. It is shown that the combined effect of thermal quasiparticle correlations and of continuum coupling washes out the sharp superfluid-normal phase transition given by the standard finite-temperature BCS calculations. Within the proposed resonant-continuum MBCS approximation the fluctuations of particle number also become more suppressed especially at high temperature for nuclei closer to the drip line. Finally, it is found within the same approximation that the two-neutron separation energy for ^{84}Ni drops to zero at $T \simeq 0.8$ MeV.

DOI: 10.1103/PhysRevC.67.014304 PACS number(s): 21.60.−n, 21.30.Fe, 24.10.Pa

I. INTRODUCTION

It is well known that there exists a sharp phase transition from the superfluid phase to the normal-fluid one in infinite Fermi systems at finite temperature. For metal superconductors [1] and nuclear matter the pairing correlations sharply vanish at the critical temperature $T_c \approx 0.567\Delta(0)$, where $\Delta(0)$ is the pairing gap at zero temperature $T=0$ [2]. This value is obtained by solving the finite-temperature BCS (FTBCS) equations for a constant level density around the chemical potential, where the pairing correlations are strong [3–5].

In finite Fermi systems, especially in small systems such as nuclei, fluctuations due to the finiteness of the system become large. Several papers took into account thermal fluctuations in the pairing field using the macroscopic Landau theory of phase transitions [6–8] or the static path approximation [9]. Their results showed that the gap $\Delta(T)$ does not collapse, but decreases with increasing temperature, and remains finite even at rather high temperature. This has been confirmed also by calculations using the particle number projection [10], as well as by the exact solution of the nuclear pairing problem [11]. Modern nuclear shell-model calculations in Ref. [12] also show that the pairing correlations do not abruptly disappear at $T \neq 0$ because of the existence of pairing fluctuations. The latter are enhanced near the BCS phase transition point and survive at $T > T_c$, where the static superfluid condensate is destroyed.

In nuclei close to the drip line, the effects of the nuclear finiteness upon its superfluid properties also show up in another aspect. As the Fermi level is close to the continuum threshold in such nuclei, with increasing the temperature, the nucleons are easily promoted into the continuum part of the single-particle spectrum, mainly into the single-particle resonant states which are trapped by the centrifugal or/and Coulomb barrier inside the nucleus. The resonant states, which become now important for the pairing correlations, have a continuous energy spreading and therefore the Pauli blocking, responsible for the superfluidity suppression at finite temperature, is less effective than for a spectrum formed only by bound states. On the other hand, the energy spreading of the resonant states diminishes the pairing correlations compared to a calculation in which the resonant states are treated like quasibound states [13,14]. As a result, the critical temperature T_c of the superfluid-normal phase transition within the FTBCS approximation [3–5] is reduced due to the finite width of resonant states [14]. However, the sharp superfluid-normal phase transition still persists within the FTBCS and FT Hartree-Fock-Bogoliubov (FTHFB) approximations due to the omission of thermal fluctuations in these studies.

Recently, an improved treatment of ground-state correlations has been proposed in Ref. [15]. This approach employs the modified quasiparticles obtained by a secondary canonical transformation of usual quasiparticles explicitly involving the quasiparticle occupation numbers. At finite temperature, the quasiparticle occupation number is described by the Fermi-Dirac distribution function and depends on the quasiparticle energy and temperature. The finite-temperature modified BCS (FTMBCS) equations have been obtained, which include the quasiparticle correlations in the thermal equilibrium. The numerical calculations have shown that the modified BCS (MBCS) approximation increases significantly the temperature of the superfluid-normal phase transition point until smearing out completely this phase transition in ^{120}Sn [15].

The aim of this paper is to combine the approaches developed in Refs. [14,15] to study how the continuum coupling and the thermal quasiparticle correlations affect together the properties of the superfluid-normal phase transition in nuclei far from stability. The paper is organized as follows. In Sec. II we summarize the main features of the BCS, the renormalized BCS (RBCS) and modified BCS (MBCS) approximations as well as their extension to finite temperature. We also present the basic features of the model, in which the coupling to single-particle resonant states in the continuum is included in the MBCS equations at finite temperature. The results of

numerical calculations are analyzed in Sec. III. The general conclusions are drawn in the last section.

II. FORMALISM

A. Pairing Hamiltonian

We consider a system of fermions described by the particle creation and destruction operators, $a^\dagger_{jm}$ and a_{jm}, in a spherical mean field, where the single-particle orbitals are labeled by the total angular-momentum quantum numbers j and m. The pairing correlations of the system is induced by an attractive two-body force with the pairing constant G. The Hamiltonian of such system is given as

$$H=\sum_{jm}\ \epsilon_j a^\dagger_{jm}a_{jm}-\frac{1}{4}G\sum_{jj'mm'}\ a^\dagger_{jm}a^\dagger_{j\tilde{m}}a_{j'\tilde{m}'}a_{j'm'}. \quad (1)$$

where the sign $\tilde{}$ stands for the time reversal operation, e.g., $a_{j\tilde{m}}=(-1)^{j-m}a_{j-m}$. Using the canonical Bogoliubov transformation from the particle operators, $a^\dagger_{jm}$ and $a_{j\tilde{m}}$, to the quasiparticle ones, $\alpha^\dagger_{jm}$ and $\alpha_{j\tilde{m}}$

$$a^\dagger_{jm}=u_j\alpha^\dagger_{jm}+v_j\alpha_{j\tilde{m}},\ \ a_{j\tilde{m}}=u_j\alpha_{j\tilde{m}}-v_j\alpha^\dagger_{jm}, \quad (2)$$

the Hamiltonian (1) is transformed into the quasiparticle representation, whose explicit form is given as [16,17]

$$H=a+\sum_j\ b_j\mathcal{N}_j+\sum_j\ c_j(\mathcal{A}^\dagger_j+\mathcal{A}_j)+\sum_{jj'}\ d_{jj'}\mathcal{A}^\dagger_j\mathcal{A}_{j'}$$
$$+\sum_{jj'}\ g_j(j')(\mathcal{A}^\dagger_j\mathcal{N}_j+\mathcal{N}_j\mathcal{A}_{j'})+\sum_{jj'}\ h_{jj'}(\mathcal{A}^\dagger_j\mathcal{A}^\dagger_j,$$
$$+\mathcal{A}_{j'}\mathcal{A}_j)+\sum_{jj'}\ q_{jj'}\mathcal{N}_j\mathcal{N}_{j'}. \quad (3)$$

Here $\mathcal{N}_j$ is the operator of the quasiparticle number on the j shell, while $\mathcal{A}^\dagger_j$ and $\mathcal{A}_j$ are the creation and destruction operators of a pair of time-conjugate quasiparticles:

$$\mathcal{N}_j=\sum_m\ \alpha^\dagger_{jm}\alpha_{jm},\ \ \mathcal{A}^\dagger_j=\frac{1}{\sqrt{\Omega_j}}\sum_{m>0}\ \alpha^\dagger_{jm}\alpha^\dagger_{j\tilde{m}},$$
$$\mathcal{A}_j=(\mathcal{A}^\dagger_j)^\dagger,\ \ \Omega_j=j+\frac{1}{2}. \quad (4)$$

They obey the following exact commutation relations:

$$[\mathcal{A}_j,\mathcal{A}^\dagger_{j'}]=\delta_{jj'}\left(1-\frac{\mathcal{N}_j}{\Omega j}\right), \quad (5)$$

$$[\mathcal{N}_j,\mathcal{A}^\dagger_{j'}]=2\delta_{jj'}\mathcal{A}^\dagger_j,\ \ [\mathcal{N}_j,\mathcal{A}_{j'}]=-2\delta_{jj'}\mathcal{A}_j. \quad (6)$$

The coefficients in Eq. (3) are

$$a=2\sum_j\ \Omega_j\epsilon_j v_j^2-G\left(\sum_j\ \Omega_j u_j v_j\right)^2-G\sum_j\ \Omega_j v_j^4, \quad (7)$$

$$b_j=\epsilon_j(u_j^2-v_j^2)+2Gu_jv_j\sum_{j'}\ \Omega_{j'}u_{j'}v_{j'}+Gv_j^4, \quad (8)$$

$$c_j=2\sqrt{\Omega_j}\epsilon_j u_j v_j-G\sqrt{\Omega_j}(u_j^2-v_j^2)\sum_{j'}\ \sqrt{\Omega_{j'}}u_{j'}v_{j'}$$
$$-2G\sqrt{\Omega_j}u_jv_j^3, \quad (9)$$

$$d_{jj'}=-G\sqrt{\Omega_j\Omega_{j'}}(u_j^2u_{j'}^2+v_j^2v_{j'}^2)=d_{j'j}, \quad (10)$$

$$g_j(j')=Gu_jv_j\sqrt{\Omega_{j'}}(u_{j'}^2-v_{j'}^2), \quad (11)$$

$$h_{jj'}=\frac{G}{2}\sqrt{\Omega_j\Omega_{j'}}(u_j^2v_{j'}^2+v_j^2u_{j'}^2)=h_{j'j}, \quad (12)$$

$$q_{jj'}=-Gu_jv_ju_{j'}v_{j'}=q_{j'j}. \quad (13)$$

B. BCS approximation

The standard BCS equation is usually obtained making use of the variational procedure to get the minimum of the average value of $H-\lambda\hat{N}$ (λ is the chemical potential, $\hat{N}=\Sigma_{jm}a^\dagger_{jm}a_{jm}$ is the particle-number operator) over the BCS ground state $|\mathrm{BCS}\rangle$, which is taken as the quasiparticle vacuum, i.e.,

$$\alpha_{jm}|\mathrm{BCS}\rangle=0. \quad (14)$$

This approximation leads to the following average values for commutator (5),

$$\langle\mathrm{BCS}|[\mathcal{A}_j,\mathcal{A}^\dagger_{j'}]|\mathrm{BCS}\rangle=\delta_{jj'}, \quad (15)$$

because the average of the quasiparticle occupation number n_j^{BCS} in the BCS ground state $|\mathrm{BCS}\rangle$ vanishes due to definition (14),

$$n_j^{\mathrm{BCS}}\equiv\langle\mathrm{BCS}|\alpha^\dagger_{jm}\alpha_{jm}|\mathrm{BCS}\rangle=\frac{1}{2\Omega_j}\langle\mathrm{BCS}|\mathcal{N}_j|\mathrm{BCS}\rangle=0. \quad (16)$$

The average value (15) means that, within the BCS approximation, the quasiparticle pair operators $\mathcal{A}^\dagger_j$ and $\mathcal{A}_j$ behave like bosons (the Cooper pairs), just violating the Pauli principle between them.

Within the BCS approximation, only the a term in Eq. (3) contributes, which leads to the well-known BCS equations to determine the gap Δ and chemical potential λ:

$$\Delta=G\sum_j\ \Omega_j u_j v_j,\quad N=2\sum_j\ \Omega_j v_j^2=\sum_j\ \Omega_j\left(1-\frac{\epsilon'_j-\lambda}{E_j}\right), \quad (17)$$

where the single-particle energy is $\epsilon'_j=\epsilon_j$ if the self-energy term $-Gv_j^2$ is neglected, or $\epsilon'_j=\epsilon_j-Gv_j^2$ if the self-energy term is included. The quasiparticle energy is $E_j=\sqrt{(\epsilon'_j-\lambda)^2+\Delta^2}$. The u_j and v_j coefficients are given as

$$u_j^2=\frac{1}{2}\left(1+\frac{\epsilon_j'-\lambda}{E_j}\right),\quad v_j^2=\frac{1}{2}\left(1-\frac{\epsilon_j'-\lambda}{E_j}\right). \tag{18}$$

The a term [Eq. (7)] is actually the ground state energy within the BCS, since this is the only term that remains in the average over the quasiparticle vacuum $|\mathrm{BCS}\rangle$, where the second term in Eq. (7) can be now replaced with $-\Delta^2/G$ using Eq. (17).

The violation of the Pauli principle within the BCS approximation due to the BCS ground state (14) causes the well-known violation of the particle-number conservation. As the result, the BCS approximation induces the following fluctuations of the particle number [17]:

$$\delta N^2=\langle \mathrm{BCS}|\hat{N}^2|\mathrm{BCS}\rangle-\langle \mathrm{BCS}|\hat{N}|\mathrm{BCS}\rangle^2=4\sum_j \Omega_j u_j^2 v_j^2$$

$$=\Delta^2\sum_j \frac{\Omega_j}{E_j^2}. \tag{19}$$

These fluctuations can be roughly estimated using a symmetric Ω-degenerate two-level model with the shell distance equal to ϵ. In this case $E_j=G\Omega$ $(\Omega=N/2)$ and $\delta N^2=2\Delta^2/(G^2N)$. Therefore, in finite small systems such as nuclei, when the particle number is not sufficiently large, the effects of particle-number fluctuations must be taken into account. The BCS equations (17) do not have a nontrivial solution below a critical value G_c of the pairing interaction strength G, at which the BCS approximation breaks down. For example, in the above-mentioned two-level model, it is easy to find that $G_c=\epsilon/(2\Omega)$ (neglecting the self-energy correction) [16] or $\epsilon/(2\Omega-1)$ (including the self-energy correction) [18], below which the BCS pairing gap Δ becomes imaginary.

C. Renormalized BCS (RBCS) approximation

A simplest way to restore the Pauli principle for the quasiparticle pair operators $\mathcal{A}_j^\dagger$ and $\mathcal{A}_j$ is to introduce a new ground state $|\overline{0}\rangle$, in which the correlations among quasiparticles lead to a nonzero value of the quasiparticle occupation number $n_j\neq 0$. By doing so, we obtain

$$\langle\overline{0}|[\mathcal{A}_j,\mathcal{A}_{j'}^\dagger]|\overline{0}\rangle=\delta_{jj'}\left(1-\frac{\langle\overline{0}|\mathcal{N}_j|\overline{0}\rangle}{\Omega_j}\right)=\delta_{jj'}(1-2n_j), \tag{20}$$

instead of the quasiboson approximation (15). Now n_j is the quasiparticle number in the correlated ground state $|\overline{0}\rangle$

$$n_j=\langle\overline{0}|\alpha_{jm}^\dagger\alpha_{jm}|\overline{0}\rangle=\frac{1}{2\Omega_j}\langle\overline{0}|\mathcal{N}_j|\overline{0}\rangle\neq 0, \tag{21}$$

instead of Eq. (16). Repeating the same variational procedure with the Hamiltonian (3) as it was done to derive the standard BCS equation, but taking into account Eq. (21), one obtains the following equations:

$$\tilde{\Delta}=G\sum_j \Omega_j u_j v_j(1-2n_j), \tag{22}$$

$$N=\sum_j \Omega_j\left[1-\frac{\epsilon_j'-\lambda}{E_j}(1-2n_j)\right]. \tag{23}$$

We shall call Eqs. (22)–(23) RBCS equations due to the renormalization factor $(1-2n_j)$, which makes the renormalized quasiparticle-pair operators $\tilde{\mathcal{A}}_j^\dagger\equiv\mathcal{A}_j^\dagger/\sqrt{1-2n_j}$ and $\tilde{\mathcal{A}}_j\equiv\mathcal{A}_j/\sqrt{1-2n_j}$ behave now like bosons. The quasiparticle occupation number n_j can be calculated approximately in terms of the backward-going amplitude Y within the renormalized RPA as described in Ref. [19]. The particle number fluctuations δN^2 (19) have now the following form [17],

$$\delta N^2=\delta N_1^2+\delta N_2^2, \tag{24}$$

where

$$\delta N_1^2=\tilde{\Delta}^2\sum_j \Omega_j\frac{1-2n_j}{E_j^2},$$

$$\delta N_2^2=2\sum_j \Omega_j\frac{n_j}{E_j^2}[(\epsilon_j'-\lambda)^2(1-n_j)+n_j\tilde{\Delta}^2]. \tag{25}$$

D. Finite-temperature BCS (FTBCS) approximation

In this section we show that a direct result of the RBCS equations (22) and (23) is the FTBCS equations.

The major assumption in the statistical approach to the theoretical description of nuclei at finite temperature is the replacement of the individual compound systems, each with a given intrinsic excitation energy and particle number, by the grand canonical ensemble of nuclei in thermal equilibrium. The nuclear temperature T $(=\beta^{-1})$ and chemical potential λ determine the average excitation energy and average particle number of the system, respectively. The probability for a quantum system to have a given eigenenergy is determined by the density matrix $\mathcal{D}$ rather than by a pure wave function. The average value $\langle\hat{\mathcal{O}}\rangle$ of an observable $\hat{\mathcal{O}}$ is given as the statistical average over the grand canonical ensemble[1]

$$\langle\hat{\mathcal{O}}\rangle=\mathrm{Tr}\{\hat{\mathcal{O}}\mathcal{D}\}. \tag{26}$$

[1]A quantum mechanical ground state $|0(\beta)\rangle$ so that $\langle 0(\beta)|\hat{\mathcal{O}}|0(\beta)\rangle=\mathrm{Tr}\{\hat{\mathcal{O}}\mathcal{D}\}$ does not exist in the physical space spanned by the eigenvectors $|j\rangle$ with eigenvalues E_j of Hamiltonian (3) because it is impossible to construct a state $|0(\beta)\rangle=\Sigma_j f_j(\beta)|j\rangle$ so that $f_j(\beta)^* f_k(\beta)=\exp(-\beta E_j)\delta_{jk}/Z$ with $f_j(\beta)$ being numbers. In order to construct such state, the founders of the thermo field dynamics [20] had to introduce a fictitious dynamical system, whose physical interpretation still remains to be clarified.

The formal solution for the density operator $\mathcal{D}$ is found from the stationary requirement for the grand potential Ω in thermal equilibrium

$$\delta\Omega/\delta\mathcal{D}=0,\ \ \Omega=\mathcal{E}-\lambda N-TS, \tag{27}$$

where $\mathcal{E}=\mathrm{Tr}\{H\mathcal{D}\}$, $N=\mathrm{Tr}\{\hat{N}\mathcal{D}\}$, and $S=-\mathrm{Tr}\{\mathcal{D}\ln\mathcal{D}\}$ are the average energy, average particle number, and entropy of the system, respectively. As the result the density operator $\mathcal{D}$ is given as

$$\mathcal{D}=Z^{-1}\mathrm{e}^{-\beta(H-\lambda\hat{N})},\ \ Z=\mathrm{Tr}\{e^{-\beta(H-\lambda\hat{N})}\},\ \ \beta=T^{-1}. \tag{28}$$

Since the quasiparticle Hamiltonian (3) can be represented as $H=\Sigma_j E_j\alpha^\dagger_{jm}\alpha_{jm}$ within the BCS approximation, the quasiparticle occupation number is defined in the average over the grand canonical ensemble as

$$n_j(\beta)=\mathrm{Tr}\{\alpha^\dagger_{jm}\alpha_{jm}\mathcal{D}\}=\frac{1}{e^{\beta E_j}+1}. \tag{29}$$

The proof that, when the residual interactions beyond the quasiparticle mean field are neglected, the occupation number $n_j(\beta)$ of independent quasiparticles is indeed determined by the Fermi-Dirac distribution (29) is given in the Appendix A. The statistical approach has been demonstrated to be overwhelmingly accurate for highly-excited nuclei.

As the quasiparticle occupation number n_j (21) is not zero within the RBCS approximation due to the contribution of residual interactions beyond the BCS approximation and random phase approximation (RPA), its statistical equivalence does not become exactly $n_j(\beta)$ at $T\neq 0$ since the latter gives zero in the zero-temperature limit. Moreover, the presence of the residual interactions also smooth out the Fermi-Dirac distribution as has been shown a long time ago by Bogoliubov and Tyablikov [4,21]. However, in the case of small quasiparticle damping due to coupling to collective degrees of freedom as in hot nuclei, such corrections are negligible as has been shown in Ref. [22]. Therefore, except for a very low-temperature region, where quantal fluctuations are important, one can neglect the effects of residual interactions on the quasiparticle correlations so that we have

$$n_j\simeq n_j(\beta)\quad \text{at}\ \ T\neq 0. \tag{30}$$

By doing so, we easily see that the RBCS equations (22) and (23) become the well-known FTBCS equations [4,5]. Thus, by using average (29) and approximation (30), the FTBCS equations also take into account a part of the effects of the Pauli principle between the quasiparticle pair operators $\mathcal{A}^\dagger_j$ and $\mathcal{A}_j$ via the thermal correlations of the quasiparticles in the grand canonical ensemble.

The factor $1-2n_j(\beta)$ effectively decreases the pairing strength with increasing the temperature until the point where the FTBCS approximation collapses. This behavior inspired speculations on the superfluid-normal phase transitions at finite temperature in nuclei. In reality, the violation of the particle-number conservation makes the FTBCS equations unreliable at high temperature. Indeed, at $T\neq 0$, the parts δN_1^2 and δN_2^2 of the particle-number fluctuations in Eq. (25) can be called the quantal and thermal fluctuations, respectively, as the former exists at $T=0$ while the latter appears only at $T\neq 0$ within approximation (29). Although, due to the renormalization factor $[1-2n_j(\beta)]$, the quantal fluctuations δN_1^2 of particle number decrease with increasing T and vanish at T_c where the BCS gap collapses, the thermal fluctuations δN_2^2 increase with increasing T [See Fig. 1(a) of Ref. [17]]. These thermal fluctuations of particle number significantly reduce the accuracy of the FTBCS approximation.

E. Modified BCS (MBCS) approximation

Because of Eq. (21), the correlated ground state $|\overline{0}\rangle$ (20) is no longer the vacuum of the BCS quasiparticle operators $\alpha^\dagger_{jm}$ and α_{jm}. A further step to improve the treatment of ground-state correlations has been taken within the MBCS approximation and the modified RPA [15]. This formalism proposes that the quasiparticles are modified by the correlations in the correlated quasiparticle ground state $|\overline{0}\rangle$ according the following secondary Bogoliubov-type canonical transformation between the quasiparticle operators, $\alpha^\dagger_{jm}$ and α_{jm}, and the modified ones, $\overline{\alpha}^\dagger_{jm}$ and $\overline{\alpha}_{jm}$:

$$\overline{\alpha}^\dagger_{jm}=U_j\alpha^\dagger_{jm}+V_j\alpha_{j\tilde{m}},\ \ \overline{\alpha}_{j\tilde{m}}=U_j\alpha_{j\tilde{m}}-V_j\alpha^\dagger_{jm}. \tag{31}$$

The coefficients U_j and V_j are normalized as usual,

$$U_j^2+V_j^2=1, \tag{32}$$

and are determined so that the average value ν_j of the modified quasiparticles in the correlated ground state $|\overline{0}\rangle$ vanishes, i.e.,

$$\nu_j\equiv\langle\overline{0}|\overline{\alpha}^\dagger_{jm}\overline{\alpha}_{jm}|\overline{0}\rangle=0. \tag{33}$$

Indeed, using the inverse transformation of Eq. (31), namely,

$$\alpha^\dagger_{jm}=U_j\overline{\alpha}^\dagger_{jm}-V_j\overline{\alpha}_{j\tilde{m}} \tag{34}$$

to calculate the quasiparticle occupation number n_j (21), we can easily see that

$$\begin{aligned} n_j&\equiv\langle\overline{0}|\alpha^\dagger_{jm}\alpha_{jm}|\overline{0}\rangle=U_j^2\langle\overline{0}|\overline{\alpha}^\dagger_{jm}\overline{\alpha}_{jm}|\overline{0}\rangle+V_j^2\langle\overline{0}|\overline{\alpha}_{j\tilde{m}}\overline{\alpha}^\dagger_{j\tilde{m}}|\overline{0}\rangle\\ &=V_j^2 \end{aligned} \tag{35}$$

because of Eq. (33). Using Eq. (35) and normalization (32), we obtain

$$V_j=\sqrt{n_j},\ \ U_j=\sqrt{1-n_j}. \tag{36}$$

The secondary transformation (31) with U_j and V_j coefficients given by Eq. (36), where n_j is the quasiparticle occupation number (21) was proposed for the first time in Ref. [15].

Using Eqs. (31) and (36) in combination with the original Bogoliubov transformation (2), one obtains the transformation from the particle operators directly to the modified quasiparticle operators in the following form [15]:

$$a^{\dagger}_{jm}=\overline{u}_j\overline{\alpha}^{\dagger}_{jm}+\overline{v}_j\overline{\alpha}_{j\tilde{m}},\quad a_{j\tilde{m}}=\overline{u}_j\overline{\alpha}_{j\tilde{m}}-\overline{v}_j\overline{\alpha}^{\dagger}_{jm}, \tag{37}$$

where the coefficients $\overline{u}_j$ and $\overline{v}_j$ are related to the conventional Bogoliubov coefficients u_j and v_j as

$$\overline{u}_j=u_j\sqrt{1-n_j}+v_j\sqrt{n_j},\quad \overline{v}_j=v_j\sqrt{1-n_j}-u_j\sqrt{n_j}. \tag{38}$$

Due to definition (33) the average value of the commutation relations between the modified quasiparticle-pair operators $\overline{\mathcal{A}}^{\dagger}_j$ and $\overline{\mathcal{A}}_j$ in the modified ground state (33) is exactly the same as Eq. (15) for the quasiparticle-pair operators $\mathcal{A}^{\dagger}_j$ and $\mathcal{A}_j$ in the BCS ground state $|\mathrm{BCS}\rangle$. The transformation of the pairing Hamiltonian (1) into the modified quasiparticles $\overline{\alpha}^{\dagger}_{jm}$ and $\overline{\alpha}_{jm}$ also has the form identical to Eq. (3) with $(\overline{u}_j,\overline{v}_j)$ replacing (u_j,v_j) and $(\overline{\alpha}^{\dagger}_{jm},\overline{\alpha}_{jm})$ replacing $(\alpha^{\dagger}_{jm},\alpha_{jm})$, respectively. The MBCS equations, therefore, has exactly the same form as the standard BCS equations (17), where the coefficients u_j and v_j are replaced with $\overline{u}_j$ and $\overline{v}_j$, i.e.,

$$\begin{aligned}\overline{\Delta}&=G\sum_j\ \Omega_j\overline{u}_j\overline{v}_j\\&=G\sum_j\ \Omega_j[(1-2n_j)u_jv_j-\sqrt{n_j(1-n_j)}(u_j^2-v_j^2)],\end{aligned} \tag{39}$$

$$\begin{aligned}N&=2\sum_j\ \Omega_j\overline{v}_j^2\\&=2\sum_j\ \Omega_j[(1-2n_j)v_j^2+n_j-2\sqrt{n_j(1-n_j)}u_jv_j],\end{aligned} \tag{40}$$

using Eq. (38). It is easy to see that the MBCS approximation suppresses completely the part $\delta\overline{N}_2^{(2)}$ for fluctuations (25) of particle number in the modified ground state $|\overline{0}\rangle$ (33). Indeed, using transformation (37) we obtain

$$\begin{aligned}\delta\overline{N}^2&\equiv\langle\overline{0}|\hat{N}^2|\overline{0}\rangle-\langle\overline{0}|\hat{N}|\overline{0}\rangle^2=4\sum_j\ \Omega_j\overline{u}_j^2\overline{v}_j^2=\overline{\Delta}^2\sum_j\ \Omega_j/\overline{E}_j^2\\&=\delta\overline{N}_1^2,\quad \delta\overline{N}_2^2=0,\end{aligned} \tag{41}$$

because of definition (33).

The quasiparticle number n_j (35), which enters Eqs. (36)–(40), in general, should be calculated self-consistently using the MBCS (or RBCS) and the modified quasiparticle RPA (MQRPA) [or renormalized QRPA (RQRPA)] equations, as has been proposed in Ref. [15]. These elaborated calculations are presented in Appendix B for both of the schemes, namely, the RBCS+RQRPA and MBCS+MQRPA ones, using the Hamiltonian (3). In Sec. 3 of Appendix B, the results of numerical calculations are compared with those obtained when n_j is replaced by the Fermi-Dirac distribution $n_j(\beta)$ of noninteracting quasiparticles (Fermi gas) [Eq. (29)]. This comparison shows that approximation (30) turns out to be very good. Therefore, we will use this approximation for all the numerical calculations in the rest of the paper.

We call the MBCS equations (39) and (40) within approximation (30) the FTMBCS equations. The expression of $\overline{u}_j$ and $\overline{v}_j$ in terms of u_j and v_j at the right-hand side (rhs) of Eqs. (39) and (40) is important to reveal the dependence of the pairing gap $\overline{\Delta}$ and the modified chemical potential $\overline{\lambda}$ on $n_j(\beta)$, i.e., on temperature T of the usual quasiparticles $\alpha^{\dagger}_{jm}$ and α_{jm} since the average is taken in the canonical ensemble of usual quasiparticles in thermal equilibrium. These equations differ from the conventional FTBCS equations (22) and (23) $[n_j=n_j(\beta)]$ by the second terms at the rhs, containing $\sqrt{n_j(\beta)[1-n_j(\beta)]}$, which take into account the correlations induced by thermal effects. The presence of the last term at the rhs of Eq. (39) increases the value $\overline{T}_c$ of the critical temperature at which the gap $\overline{\Delta}$ vanishes. Indeed, the critical temperature $\overline{T}_c$ is determined as the value of T at which $\Sigma_j\Omega_j\sqrt{n_j(\beta)[1-n_j(\beta)]}(u_j^2-v_j^2)$ is positive and becomes equal to $\Sigma_j\Omega_ju_jv_j[1-2n_j(\beta)]$, depending on the shell structure of the given single-particle energy spectrum. Since the absolute value of the last term at the rhs of Eq. (39) is suppressed largely due to the factor $\sqrt{n_j(\beta)[1-n_j(\beta)]}$, which is much smaller than $(1-2n_j)$ in the low-temperature region, it is easy to see that $\overline{T}_c>T_c$. At $T>\overline{T}_c$, the gap $\overline{\Delta}(\beta)$ (39) becomes negative and the results given by the FTMBCS are no longer reliable. Finally, based on Eqs. (41) we also see that the FTMBCS equations suppress completely the thermal fluctuations $\delta\overline{N}_2^2(\beta)$ of the particle number.

F. Coupling to continuum single-particle states

The extension of the conventional FTBCS equations to include the contribution of the continuum single-particle states has been performed in Ref. [14]. The treatment of both continuum and temperature effects in stationary models such as the BCS approximation is complicated by the fact that the particles scattered in the continuum are permanently emitted from the nucleus, producing a nucleonic gas in thermal equilibrium with the nucleus. Therefore, in order to calculate the quantities related to the nucleus itself, the contribution of the nucleonic gas should be subtracted [23]. As discussed in Ref. [14], within the BCS approximation this can be done by evaluating the contribution of the continuum by the continuum level density $g(\epsilon)$ defined by

$$g(\epsilon)=\frac{2}{\pi}\sum_j\ \Omega_j\frac{d\delta_j}{d\epsilon}, \tag{42}$$

where δ_j is the phase shift related to the nuclear mean field. Therefore the FTBCS equations with continuum coupling can be obtained by writing formally the FTBCS equations (22) and (23) $[n_j=n_j(\beta)]$ in terms of the bound states level density $g_b(\epsilon)$ and then replacing $g_b(\epsilon)$ by the total level density, i.e., $g_b(\epsilon)+g(\epsilon)$.

Using the same prescription we can also include the effect of the continuum coupling into the FTMBCS equations (39) and (40) with $n_j=n_j(\beta)$:

$$\tilde{\Delta}=G\Bigg\{\sum_j \Omega_j[(1-2n_j)u_jv_j-\sqrt{n_j(1-n_j)}(u_j^2-v_j^2)] + \frac{1}{2}\int g(\epsilon)\{[1-2n(\epsilon)]u(\epsilon)v(\epsilon)-\sqrt{n(\epsilon)[1-n(\epsilon)]} \times[u^2(\epsilon)-v^2(\epsilon)]\}d\epsilon\Bigg\}, \quad (43)$$

$$N=2\sum_j \Omega_j[(1-2n_j)v_j^2+n_j-2\sqrt{n_j(1-n_j)}u_jv_j] + \int g(\epsilon)\{[1-2n(\epsilon)]v^2(\epsilon)+n(\epsilon) -2\sqrt{n(\epsilon)[1-n(\epsilon)]}u(\epsilon)v(\epsilon)\}d\epsilon, \quad (44)$$

where $n(\epsilon)$ is obtained from $n_j(\beta)$ replacing the discrete single-particle energy ϵ_j with the integration parameter ϵ. In a similar way we can now introduce the continuum contribution to the total energy $\mathcal{E}$ of the system, calculated within the FTMBCS approximation,

$$\mathcal{E}=2\sum_j \Omega_j\epsilon_j[(1-2n_j)v_j^2+n_j-2\sqrt{n_j(1-n_j)}u_jv_j] + \int g(\epsilon)\epsilon\{[1-2n(\epsilon)]v^2(\epsilon)+n(\epsilon) -2\sqrt{n(\epsilon)[1-n(\epsilon)]}u(\epsilon)v(\epsilon)\}d\epsilon-\tilde{\Delta}^2/G, \quad (45)$$

where ϵ_j are the single-particle energies, supposed here to be temperature independent quantities. This assumption is supported by the Hartree-Fock (HF) calculations at finite temperature, which show that for $T\leqslant 5$ MeV the variation of the single-particle energies with the temperature is negligible [23,24]. The excitation energy E^* is defined using Eq. (45) as

$$E^*=\mathcal{E}(T)-\mathcal{E}(0). \quad (46)$$

As has been pointed out in Ref. [13], although one starts with a constant pairing interaction, in the resonant-continuum BCS equations the variation of the matrix elements of the interaction in the energy region of a resonance is in fact taken into account through the continuum level density $g(\epsilon)$. This effect, related to the width of resonant states, is lost if the continuum is replaced by a set of discrete states, e.g., as selected by a box of finite radius. One should notice also that in the equations above the continuum level density cancels the contribution of the nonresonant continuum, for which the derivative of the phase shift is practically zero. The continuum usually contributes through a few narrow and well separated resonant states [13,14]. Therefore, one can replace in the equations above the continuum level density with

TABLE I. Neutron single-particle states used in calculations for $^{68-84}$Ni isotopes.

Shell	State	ϵ_j (MeV)	$\Gamma_j/2$ (MeV)
	$1g_{7/2}$	4.229	0.171
50–82	$2f_{7/2}$	3.937	1.796
	$1h_{11/2}$	3.334	0.014
	$2d_{3/2}$	1.338	0.489
	$3s_{1/2}$	−0.284	
	$2d_{5/2}$	−0.80	
28–50	$1g_{9/2}$	−4.398	
	$1f_{5/2}$	−5.623	
	$2p_{1/2}$	−5.649	
	$2p_{3/2}$	−7.836	

$$g(\epsilon)=\frac{1}{\pi}\sum_j (2j+1)\frac{\frac{1}{2}\Gamma_j}{(\epsilon-\epsilon_j)^2+\left(\frac{1}{2}\Gamma_j\right)^2}, \quad (47)$$

where ϵ_j and Γ_j are the energy and the width of the resonance state with angular momentum j, respectively. One notices that in the limit of zero widths, the rhs of Eq. (47) becomes a sum of δ functions, recovering the level density of the bound spectrum. The numerical calculations discussed in the following section are obtained with the integration in Eqs. (43)–(45) carried out within the region near the single-particle resonances, which is defined as $|\epsilon-\epsilon_j|\leqslant 2\Gamma_j$.

III. NUMERICAL RESULTS

In order to illustrate how the continuum and the thermal quasiparticle correlations affect the properties of open-shell nuclei far from β-stability line, we solved the FTMBCS equations plus continuum coupling (43) and (44), discussed in the preceding section, for neutron-rich Ni isotopes. We analyze how the pairing correlations are changing when a few neutrons are subtracted or added to the doubly closed-shell nucleus ^{78}Ni, which is the heaviest Ni isotopes produced at present. Since all the calculations are performed at finite temperature, we drop the prefix ''FT'' when addressing to the FTBCS and FTMBCS equations hereafter.

The neutron single-particle states used in the present calculations are shown in Table I. They were calculated using a Woods-Saxon potential with the depth $V_0=40$ MeV, radius $R_0=1.27$ fm, and surface thickness $a=0.67$ fm. For the spin-orbit interaction we use a Woods-Saxon potential with the same values for the radius R_0 and surface thickness a, but the depth is changed to the value $V_{so}=21.43$ MeV. These parameters are chosen so that the obtained single-particle spectrum for ^{78}Ni is similar to that given by the Skyrme-HF calculations [13]. The calculations used the single-particle energies $\epsilon_j'=\epsilon_j$ in Eqs. (17), neglecting the self-energy correction $-Gv_j^2$, as its effect on the gap at $T\neq 0$ turns out to be negligible [15]. As seen in Table I, the structure of the standard major shell 50–82 is drastically changed close to the drip line. Thus from all five states which typically form

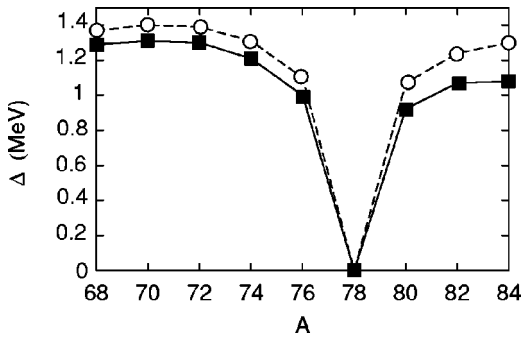

FIG. 1. Pairing gaps for Ni isotopes calculated at zero temperature within the quasibound BCS (open circles) and resonant-continuum BCS (full squares). The dashed and solid lines are drawn to guide the eyes.

this major shell, only two states, $2d_{5/2}$ and $3s_{1/2}$, are bound, while the rest of the three states, $2d_{3/2}$, $1h_{11/2}$, and $1g_{7/2}$, are resonant states. Moreover, we can see that the state $2f_{7/2}$, which usually belongs to the next major shell, appears now as a resonant state with energy below the state $1g_{7/2}$. The widths of these resonant states are shown in the fourth column of Table I. Their effects on the pairing correlations, both in resonant-continuum BCS and MBCS equations, appear through the continuum level density. In order to see these effects we perform also a calculation, in which the resonant states are treated as quasibound states, i.e., replacing in the BCS equations the continuum level density with the Dirac δ function. These calculations will be quoted below as quasibound BCS and quasibound MBCS. The pairing matrix elements are considered equal with the constant G in all the calculations. We chose for G the value 0.214 MeV. This value gives within the quasibound BCS a pairing gap of 1.3 MeV for ^{84}Ni at $T=0$, as in Ref. [14]. The pairing gaps at $T=0$ obtained for the sequence of Ni isotopes under consideration are plotted in Fig. 1. As can be seen in this figure, the gaps are reduced by including the effect of the widths of resonant states in the BCS equations, in agreement with the previous findings [14]. The same reduction of the gap due to the finite widths of the resonant states is observed at finite temperature, as shown in Fig. 2. As expected, this effect is enhanced in the vicinity of the drip line, but for all the isotopes shown in Fig. 2, the curves $\Delta(T)$ obtained within the resonant-continuum BCS and quasibound BCS are almost parallel to each other. Moreover, although the critical temperature is significantly diminished due to the finite widths of the resonant states, the ratio $T_c/\Delta(0)$ remains close to 0.57 in both calculations.

The situation changes when together with the continuum coupling we introduce the effect of the thermal quasiparticle correlations. From Fig. 2 one can see that, as compared with the quasibound BCS, the quasibound-modified BCS predicts a slower decrease of pairing gap with increasing temperature, as has been noticed previously in the calculations using a bound spectrum within the MBCS approximation [15]. The sharp superfluid-normal phase transition occurs at a much higher temperature $\overline{T}_c \gg T_c$. However, as the thermal quasiparticle correlations decrease with increasing the particle number, the slopes of two curves are getting closer. For ^{84}Ni, in the temperature range 0.5 MeV $\leqslant T \leqslant 0.6$ MeV, the gap obtained within the quasibound-MBCS drops even faster than that given by the quasibound BCS.

Taking the widths of the resonant states into account, the MBCS predicts a slower decrease of the gap than that given by the quasibound MBCS as the temperature increases. This is due to the fact that, with the increasing temperature, the Pauli blocking becomes less effective due to the spreading of the resonant states. The gap obtained within the resonant-continuum MBCS remains finite as a long tail extended to $T>2$ MeV. In general, we found that by introducing the width of the resonances into the MBCS equations the sharp superfluid-normal phase transition is washed out for all the isotopes under consideration. As seen in Fig. 2, for the isotopes close to the drip line, ^{82,84}Ni, the gap remains finite at high temperatures, far beyond the critical temperature predicted by the quasibound-MBCS calculations. At such high temperatures the Fermi distribution becomes smooth and covers more and more levels in the valence shell 50–82 as well as in the major shell 28–50 so that the latter starts to contribute significantly to the pairing correlations. This can be seen in Fig. 3(a), which displays the pairing gap calculated after removing one, two, three, and all four levels from the major shell 28–50, starting from the lowest level. The constant G is changed so that the gap remains the same for all the calculations at zero temperature. The results show that the coupling to a smaller number of bound states in the shell 28–50 decreases the critical temperature of the superfluid-normal phase transition back to a value close to that obtained within the quasibound BCS.

The contribution of the major shell 28–50 to the pairing correlations increases with the temperature, and therefore the actual value of the gap can also increase at high temperatures, if the Pauli blocking is not very strong. This effect can be seen in Fig. 3(b), where the gap in ^{84}Ni increases from 0.06 MeV at $T=1.5$ MeV to a value of 0.2 MeV at $T=6$ MeV. As shown also in Fig. 3(b), this effect can be made more evident by artificially reducing the energy of the lowest resonant state $2d_{3/2}$. This numerical test shows that the effect of gap increase at high temperature may be stronger for those drip line nuclei which have a resonant state close to the continuum threshold.

The MBCS equations (39) and (43) also suggest that, in principle, thermal effects may induce pairing correlations even for doubly closed-shell nucleus at finite temperature. In fact, for ^{78}Ni, we found that, within the resonant-continuum MBCS, the gap becomes nonzero at $T\neq 0$, increases with increasing T to reach its maximal value equal to around 0.07 MeV at $T=0.68$ MeV, then decreases again to vanish at $T=1.2$ MeV. However, a maximal value of 0.07 MeV of the pairing gap cannot be considered to be physically significant.

Shown in Fig. 4 is the temperature dependence of the excitation energy E^*. The slope of the excitation energy is slightly smaller within the quasibound BCS, where the effect of the width of resonant states is neglected, as has been discussed previously in Ref. [14]. Within the resonant-continuum MBCS, the persistence of the pairing gap at high temperature significantly reduces the excitation energy. Al-

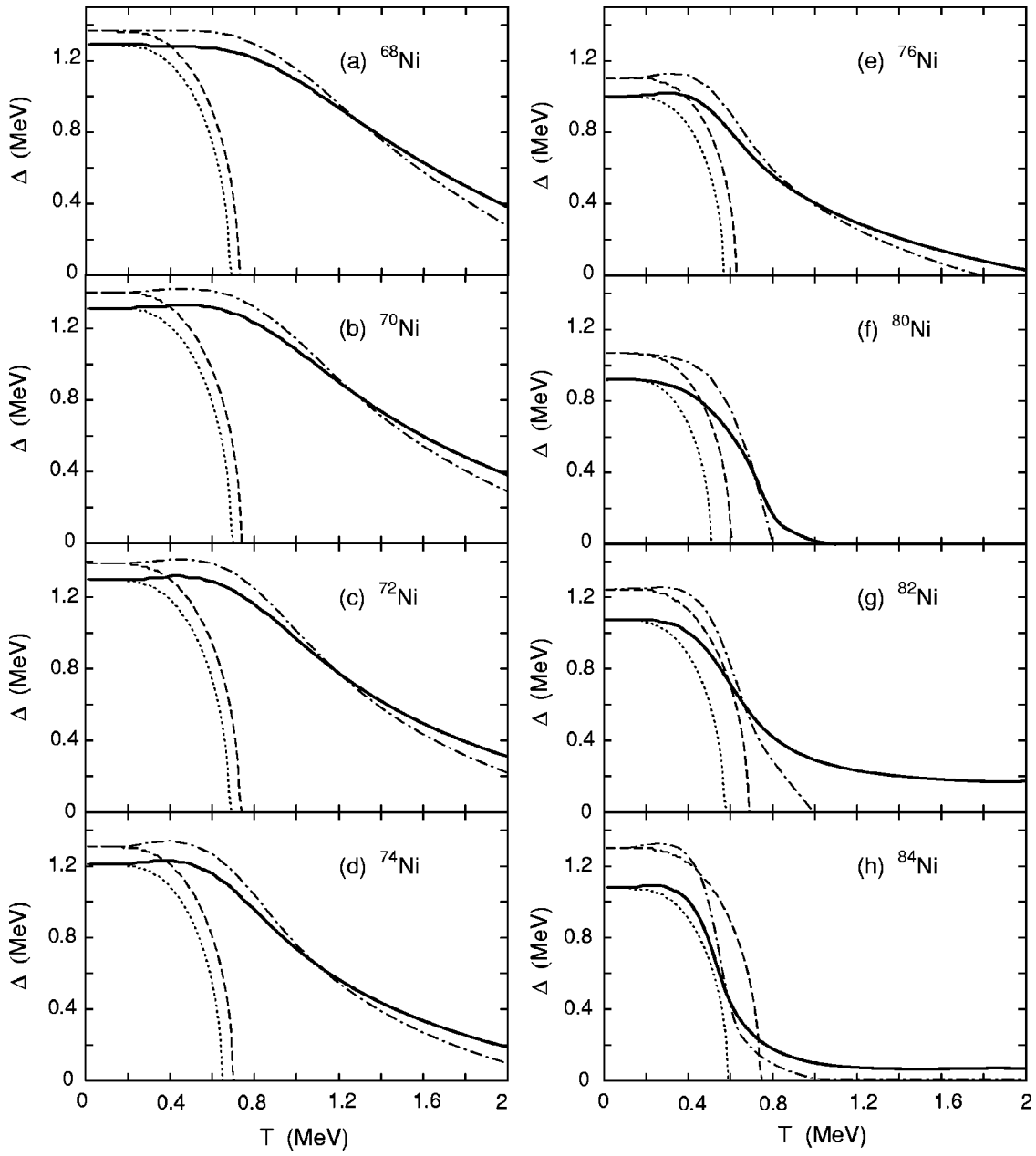

FIG. 2. Pairing gaps for Ni isotopes as a function of temperature. The dashed, dotted, dash-dotted, and solid lines represent the solutions of the quasibound BCS, resonant-continuum BCS, quasibound MBCS, and resonant-continuum MBCS, respectively.

though the difference between different approximations under consideration in the excitation energy is reduced upon increasing the mass number A, there remains a clear effect of coupling to the continuum in at high temperature for all isotopes under consideration.

The temperature dependences of the particle-number fluctuations $\sqrt{\delta N_i^2}$ $(i=1,2)$ within the BCS and the resonant-continuum MBCS approximations for ^{70,76,84}Ni are displayed in Fig. 5. The quantal fluctuations of particle number ($i=1$) decrease and vanish at $T=T_c$ while the thermal fluctuations of particle number ($i=2$) increase with increasing T within the standard BCS approximation, as has been discussed in Secs. II D, II E, and Ref. [17]. Meanwhile, within the MBCS approximation, only $\sqrt{\delta N_1^2}$ survives, which decreases with increasing T. In nuclei close to the drip line, the particle-number fluctuations are more suppressed within the MBCS approximation especially at high temperature.

A particular interest in the study of unstable nuclei is the identification of the location of the two-neutron drip line. One of the quantities that provide the relevant information of the two-neutron drip line is the two-neutron separation energy S_{2n}, defined as the difference between the energy for the $(N-2)$- and N-neutron systems with the same proton number, i.e., $S_{2n}=\mathcal{E}(N-2,Z)-\mathcal{E}(N,Z)$ [25]. A nucleus with N neutrons is unstable against the emission of a neutron pair if S_{2n} becomes negative. The nucleus is then beyond the two-neutron drip line. Using this quantity, it has been found by the recent continuum Hartree-Fock-Bogoliubov (HFB)

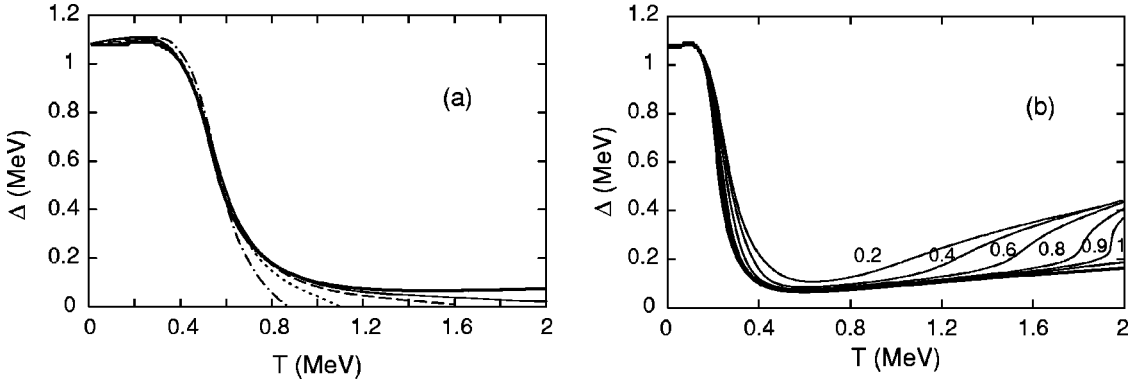

FIG. 3. Pairing gap for ^{84}Ni obtained within the resonant-continuum MBCS as a function of temperature. The thick solid line is the same as in Figs. 2(h). In (a), the thin, dashed, dotted, and dash-dotted lines are results obtained after removing one, two, three, and all four levels from the major shell 28–50, respectively, starting from the lowest level. The thin solid lines in (b) represent the results obtained using the single-particle spectrum from Table I, in which the energy of the lowest resonant state is reduced to 1, 0.9, 0.8, 0.6, 0.4, and 0.2 MeV, as indicated on the curves, respectively.

calculations in Ref. [26] that the heaviest bound Ni isotope is ^{86}Ni.

The two-neutron separation energies S_{2n} calculated within the BCS and MBCS approximations are plotted in Figs. 6(a) and 6(b), respectively, against the mass number A for the Ni isotopes under consideration at several temperatures. The coupling to the continuum via the widths of the resonant states are taken into account in both approximations. The results obtained within the quasibound BCS and quasibound MBCS are very similar to those shown in this figure. It is seen that the decrease of S_{2n} with increasing A is smoother within the MBCS approximation than the BCS one, especially with increasing temperature. This is a direct consequence of the smooth temperature dependence of the pairing gap within the MBCS discussed previously. A particular interesting feature revealed by this figure is the reduction of two-neutron separation energy with increasing T within the MBCS approximation for the isotopes close to the drip line. Thus, the value of S_{2n} for ^{84}Ni drops from around 1 MeV at $T=0.3$ MeV to almost zero at $T=0.8\sim1$ MeV [see Fig. 6(b)]. This does not happen within the BCS approximation [See Fig. 6(a)]. This observation suggests that thermal quasiparticle correlations, which are taken into account within the MBCS approximation, may cause the drip line to be reached earlier in mass units at finite temperature. In the present example, the two-neutron drip line is reached at ^{84}Ni, i.e., at two mass units earlier, at $T=0.8\sim1$ MeV.

IV. CONCLUSIONS

In this paper we have studied how the thermal quasiparticle fluctuations and the continuum coupling affect the pairing correlations in neutron-rich Ni isotopes. The thermal quasiparticle correlations are introduced making use of a secondary canonical Bogoliubov-type transformation, which defines the modified quasiparticle operators. The latter depends on temperature via the usual quasiparticle occupation number, which is approximated by a Fermi-Dirac distribution. In addition, the coupling to the continuum is introduced into the BCS approximation via a few low-lying resonant states taking into account the effect of their widths in terms of the continuum level density. The calculations of the pairing gap and excitation energy have been done for neutron-rich isotopes $^{68-84}$Ni. The results show that the combined effect of the thermal quasiparticle correlations and of continuum coupling reduces the pairing gap in the low-temperature region and washes out the sharp superfluid-normal phase transition found in the standard FTBCS and FTHFB calculations, which neglect these effects. We noticed that at high temperatures the smooth decrease of the gap is partially caused by the spreading width of resonant states, which make the Pauli blocking less effective. The fluctuations of particle number are also more suppressed within the resonant-continuum MBCS approximation, especially at high temperature and for nuclei closer to the drip line. The results obtained suggest that it is more reliable to use the proposed approximation rather than the conventional FTBCS (or FTHFB) formalism for the study of superfluid properties of nuclei close to the drip line at finite temperature.

Two interesting features, from our point of view, have been observed within this work. The first feature is that the two-neutron separation energy obtained within the MBCS approximation for ^{84}Ni reaches zero at temperature around $T=0.8\sim1$ MeV. This suggests that the thermal quasiparticle fluctuations may cause the drip line to be reached earlier in mass units compared to the zero-temperature case. The second feature is a weak increase of the pairing gap with increasing temperature at $T>1.5$ MeV for nuclei close to the drip line, and the enhancement of this effect when the energy of the lowest resonant state is artificially pushed close to zero. These observations may serve as a hint to search for stronger effects of this kind in drip line nuclei at finite temperature.

ACKNOWLEDGMENTS

The authors are grateful to Dr. N. Sandulescu for his invaluable assistance in numerical calculations and many fruitful discussions during the preparation of the manuscript. N.D.D. thanks Professor B. Mottelson for invaluable discussions and comments regarding this work.

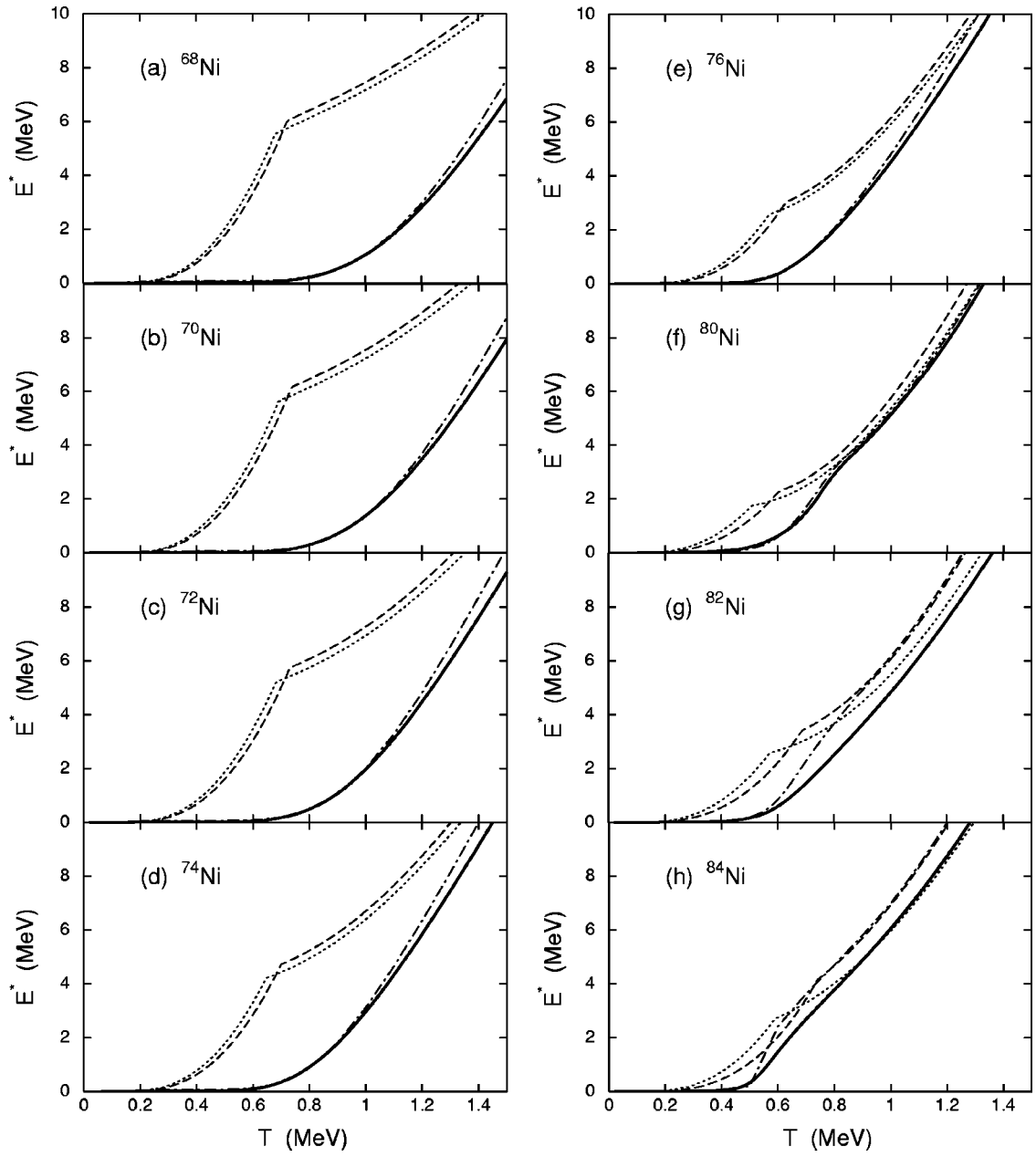

FIG. 4. Excitation energies for Ni isotopes as a function of temperature. The notations are as in Fig. 2.

APPENDIX A: OCCUPATION NUMBER FOR INDEPENDENT QUASIPARTICLES

This appendix summarizes the derivation for the quasiparticle occupation number $n_j(\beta)$ at finite temperature (29), which was given for the first time in Ref. [4].

We consider the Hamiltonian of noninteracting quasiparticles with energies E_j in the form

$$H=\sum_j E_j\alpha^\dagger_{jm}\alpha_{jm}, \tag{A1}$$

and introduce for them the double-time retarded Green function $G_j(t-t')$ as [4]

$$G_j(t-t')=-i\,\theta(t-t')\langle\{\alpha_j(t),\alpha^\dagger_j(t')\}\rangle, \tag{A2}$$

where $\langle\cdots\rangle$ is the average over the grand canonical ensemble (26) with density operator (28). The sign $\{\ldots,\ldots\}$ denotes the fermion commutator (anticommutator). The magnetic quantum number m is omitted as the result does not depend on it. The equation of motion for the Green function (A2) is given following the standard method of double-time Green functions [4] as

$$i\frac{dG_j(t-t')}{dt}=\delta(t-t')+E_jG_j(t-t'). \tag{A3}$$

Making the Fourier transform

$$G_j(t-t')=\int_{-\infty}^{\infty}G_j(E)e^{-iE(t-t')}dE, \tag{A4}$$

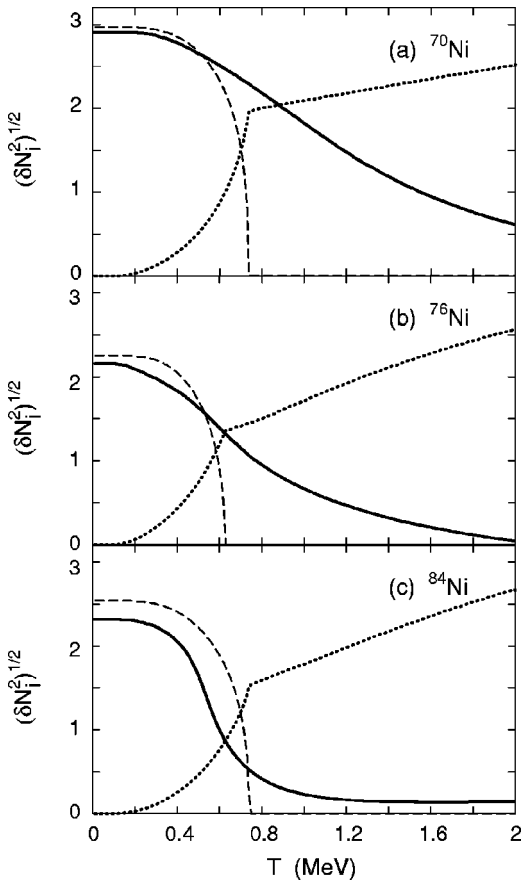

FIG. 5. Particle-number fluctuations $\sqrt{\delta N_i^2}$ for ^{70,76,84}Ni as a function of temperature. The dashed and dotted line show $\sqrt{\delta N_1^2}$ and $\sqrt{\delta N_2^2}$, respectively, within the BCS. The solid line stands for $\sqrt{\delta N_1^2}$ within the resonant-continuum MBCS.

and using the integral representation for δ function

$$\delta(t-t')=\frac{1}{2\pi}\int_{-\infty}^{\infty}e^{-iE(t-t')}dE, \tag{A5}$$

one finds

$$G_j(E)=\frac{1}{2\pi}\frac{1}{E-E_j}. \tag{A6}$$

Using the spectral representation for the retarded Green function (A2), one obtains

$$G_j(\omega+i\varepsilon)-G_j(\omega-i\varepsilon)=-i(e^{\beta\omega}+1)J_j(\omega), \tag{A7}$$

where ω is real, $\varepsilon\to 0$ $(\varepsilon>0)$, and $J_j(\omega)$ is the spectral intensity, which defines the time correlation function for quasiparticles as

$$\mathcal{F}_j(t-t')=\langle\alpha_j^\dagger(t')\alpha_j(t)\rangle=\int_{-\infty}^{\infty}J_j(\omega)e^{-i\omega(t-t')}d\omega. \tag{A8}$$

Inserting $J_j(\omega)$ from Eq. (A7) to Eq. (A8) and using the δ-function representation

$$\delta(x)=\frac{1}{2\pi i}\left(\frac{1}{x-i\varepsilon}-\frac{1}{x+i\varepsilon}\right), \tag{A9}$$

one finds

$$\langle\alpha_j^\dagger(t')\alpha_j(t)\rangle=\frac{e^{-iE_j(t-t')}}{e^{\beta E_j}+1}. \tag{A10}$$

By setting $t=t'$ in Eq. (A10), one obtains the Fermi-Dirac distribution for the average quasiparticle number $n_j(\beta)$ in Eq. (29).

APPENDIX B: SELF-CONSISTENT CALCULATIONS OF QUASIPARTICLE OCCUPATION NUMBER

1. QRPA, RQRPA, and MQRPA equations

a. The QRPA

The standard QRPA operators, called phonon operators, have the following form in the present pairing Hamiltonian (3):

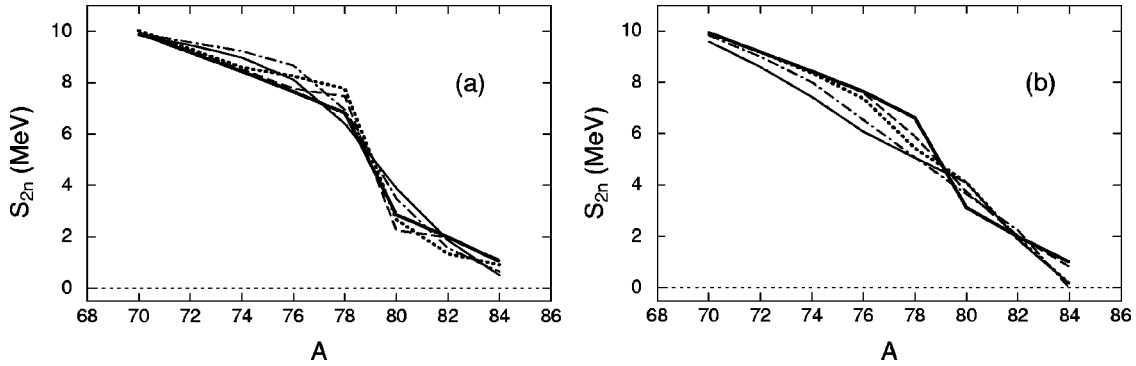

FIG. 6. Two-neutron separation energies as a function of the mass number A for Ni isotopes at temperatures $T=0.3$ (thick solid line), 0.5 (dashed line), 0.6 (dotted line), 0.8 (dash-dotted line), and 1 MeV (thin solid line). (The lines are drawn just to connect the points at given values of A in order to make the trend more visible). The results obtained within the resonant-continuum BCS and resonant-continuum MBCS are shown in (a) and (b), respectively.

$$Q_\nu^\dagger = \sum_j \left(X_j^{(\nu)} \mathcal{A}_j^\dagger - Y_j^{(\nu)} \mathcal{A}_j\right), \quad Q_\nu = (Q_\nu^\dagger)^\dagger, \tag{B1}$$

where $\mathcal{A}_j^\dagger$ and $\mathcal{A}_j$ are defined in Eq. (4). The QRPA ground state $|\mathrm{QRPA}\rangle$ is defined as the vacuum for the phonon operator, i.e., $Q_\nu|\mathrm{QRPA}\rangle = 0 = \langle \mathrm{QRPA}|Q_\nu^\dagger$. The 0^+ excited state $|0^+\rangle$ is obtained by acting $Q_\nu^\dagger$ on this vacuum, i.e., $|0^+\rangle = Q_\nu^\dagger|\mathrm{QRPA}\rangle$. The excitation energy ω_ν of the state $|0^+\rangle$, and the amplitudes $X_j^{(\nu)}$ and $Y_j^{(\nu)}$ are found, respectively, as the eigenenergy and the components of the eigenvector of the QRPA equation, which is derived from the following equation of motion for the Hamiltonian (3):

$$\langle \mathrm{QRPA}|[\delta Q, [H, Q_\nu^\dagger]]|\mathrm{QRPA}\rangle = \omega_\nu \langle \mathrm{QRPA}|[\delta Q, Q_\nu^\dagger]|\mathrm{QRPA}\rangle. \tag{B2}$$

In the standard way of derivation of the QRPA equations, the BCS equation is solved first. Then the *a* and *b* terms in the Hamiltonian (3) are replaced with the BCS result, which is $H_{\mathrm{BCS}} = \Sigma_j E_j \mathcal{N}_j$. Using the exact commutation relations (5) and (6), we see that, among the remaining terms of Eq. (3), which do not contribute in the BCS, the *d*, *h*, and *q* terms start to contribute within the QRPA. The *c* term and *g* term do not contribute since, in the commutation with the phonon operators (B1), the former gives a number, while the latter leads to the terms $\sim \mathcal{A}_j^\dagger \mathcal{A}_{j'}^\dagger$, $\sim \mathcal{A}_j^\dagger \mathcal{A}_{j'}$, and $\mathcal{N}_j(1 - \mathcal{N}_{j'}/\Omega_{j'})$, which are left out by linearizing the equation of motion according to Eq. (B2). Moreover, in order to obtain a set of QRPA equations, linear with respect to the $X_j^{(\nu)}$ and $Y_j^{(\nu)}$ amplitudes, another approximation called the quasiboson approximation is made, which implies that the following approximate commutation relation holds,

$$[\mathcal{A}_j, \mathcal{A}_{j'}^\dagger] = \delta_{jj'} \tag{B3}$$

instead of Eq. (5). The definition of phonon operators (B1) and the quasiboson approximation (B3) lead to the well-known normalization of the QRPA $X_j^{(\nu)}$ and $Y_j^{(\nu)}$ amplitudes,

$$\sum_j \left[X_j^{(\nu)} X_j^{(\nu')} - Y_j^{(\nu)} Y_j^{(\nu')}\right] = \delta_{\nu\nu'}, \tag{B4}$$

so that the phonon operators are bosons, i.e.,

$$[Q_\nu, Q_{\nu'}^\dagger] = \delta_{\nu\nu'}. \tag{B5}$$

The quasiboson approximation (B3) shows that the quasiparticle-pair operators $\mathcal{A}_j^\dagger$ and $\mathcal{A}_j$ behave like boson operators when interacting with each other. The effect of the Pauli principle represented by the last term at the rhs of Eq. (5) is just ignored. The set of QRPA equations obtained in this way is written in the matrix form as

$$\begin{pmatrix} A & B \\ -B & -A \end{pmatrix} \begin{pmatrix} X \\ Y \end{pmatrix} = \omega \begin{pmatrix} X \\ Y \end{pmatrix}, \tag{B6}$$

where the explicit form of the matrices *A* and *B* is given as

$$A_{jj'} = 2(E_j + 2q_{jj})\delta_{jj'} + d_{jj'}, \quad B_{jj'} = 2\left(1 - \frac{1}{\Omega_j}\delta_{jj'}\right) h_{jj'}. \tag{B7}$$

b. The RQRPA

The collapse of the BCS approximation and QRPA has the same origin of neglecting the Pauli principle between quasiparticle pairs operators in the BCS approximation [Eq. (15)] and the quasiboson approximation (B3). The Lipkin-Nogami method [27] approximately corrects this inconsistency within the BCS approximation. For the QRPA this is done by the RQRPA.

The essence of the RQRPA is to replace the quasiboson approximation in the form of Eq. (B3) with the average value of the commutator

$$\langle \mathrm{RQRPA}|[\mathcal{A}_j, \mathcal{A}_{j'}^\dagger]|\mathrm{RQRPA}\rangle = D_j \delta_{jj'}, \quad D_j = 1 - 2n_j^0, \tag{B8}$$

in a new ground state $|\mathrm{RQRPA}\rangle$, where the correlations beyond the QRPA due to the fermion structure of the quasiparticle pairs $\mathcal{A}_j^\dagger$ and $\mathcal{A}_j$ are taken into account, namely,

$$n_j^0 = \frac{1}{2\Omega_j}\langle \mathrm{RQRPA}|\mathcal{N}_j|\mathrm{RQRPA}\rangle \neq 0. \tag{B9}$$

The phonon operators are renormalized as

$$\mathcal{Q}_\nu = \sum_j \frac{1}{\sqrt{D_j}}\left(\mathcal{X}_j^{(\nu)} \mathcal{A}_j^\dagger - \mathcal{Y}_j^{(\nu)} \mathcal{A}_j\right), \quad \mathcal{Q}_\nu = (\mathcal{Q}_\nu^\dagger)^\dagger, \tag{B10}$$

so that the condition for phonons to be bosons within the correlated ground state $|\mathrm{RQRPA}\rangle$

$$\langle \mathrm{RQRPA}|[\mathcal{Q}_\nu, \mathcal{Q}_{\nu'}^\dagger]|\mathrm{RQRPA}\rangle = \delta_{\nu\nu'} \tag{B11}$$

leads to the same normalization condition for the amplitudes $\mathcal{X}_j^{(\nu)}$ and $\mathcal{Y}_j^{(\nu)}$ as that of the QRPA, i.e., $\Sigma_j(\mathcal{X}_j^{(\nu)}\mathcal{X}_j^{(\nu')} - \mathcal{Y}_j^{(\nu)}\mathcal{Y}_j^{(\nu')}) = \delta_{\nu\nu'}$. The factor D_j is calculated according to the approximation in Refs. [15,19] as

$$D_j = \frac{1}{1 + (\mathcal{Y}_j^{(\nu)})^2/\Omega_j}. \tag{B12}$$

The RQRPA matrices $A_{jj'}$ and $B_{jj'}$ are given as

$$A_{jj'} = 2(E_j + 2q_{jj})\delta_{jj'} + 4\sum_{j''} \Omega_{j''} q_{j'j''}(1 - D_{j''}) + D_j d_{jj'}, \tag{B13}$$

$$B_{jj'} = 2\left(D_j - \frac{1}{\Omega_j}\delta_{jj'}\right) h_{jj'}. \tag{B14}$$

c. The MQRPA

The modified RPA (MRPA) has been proposed in Ref. [15]. Its quasiparticle representation is called the modified

QRPA (MQRPA). The MQRPA equations have the same form as that of the QRPA ones given in Eqs. (B6) and (B7), but with coefficients u_j and v_j replaced with $\overline{u_j}$ and $\overline{v_j}$ [Eq. (38)], where $n_j = n_j^0$ (B9) [15]. The quasiparticle occupation number n_j^0 (B9) is found by solving self-consistently the set of RBCS+RQRPA or MBCS+MQRPA equations.

2. Quasiparticle occupation number at finite temperature

At $T=0$ coefficients $\overline{u_j}$ and $\overline{v_j}$ take the form

$$\overline{u_j^0} = u_j\sqrt{1-n_j^0} + v_j\sqrt{n_j^0}, \quad \overline{v_j^0} = v_j\sqrt{1-n_j^0} - u_j\sqrt{n_j^0}, \tag{B15}$$

where n_j^0 is defined in the preceding section. The physics of this transformation is that the Bogoliubov coefficients u_j and v_j are renormalized due to the quantal fluctuations of particle number resulting in a nonzero value of n_j^0. It is well-known that the Lipkin-Nogami method [27] is an alternative approximation to take into account such kind of renormalization. If n_j^0 is zero or negligible, the standard Bogoliubov coefficients u_j and v_j are recovered from Eq. (B15) and transformation (37) becomes the usual Bogoliubov transformation (2). The results of Ref. [17] have shown that the quantal fluctuations of particle number due to nonzero n_j^0 decreases with increasing T, while the thermal fluctuations of particle number due to the thermal distribution of quasiparticles according to the Fermi-Dirac distribution increases with increasing T. It is also well-known that at $T>2$ MeV the quasiparticles in the system described by the pairing Hamiltonian (3) behave like a pure Fermi gas. Assuming that the correction n_j^0 of the BCS approximation is small, we can approximate Eq. (38) by the following expressions:

$$\overline{u_j} \simeq u_j^0\sqrt{1-n_j(\beta)} + v_j^0\sqrt{n_j(\beta)},$$

$$\overline{v_j} \simeq v_j^0\sqrt{1-n_j(\beta)} - u_j^0\sqrt{n_j(\beta)}, \tag{B16}$$

where $n_j(\beta)$ is given by the Fermi-Dirac distribution (29). With this ansatz $\overline{u_j}$ and $\overline{v_j}$ become $\overline{u_j^0}$ and $\overline{v_j^0}$ at zero temperature since $n_j(\beta)=0$ at $T=0$. Inserting Eqs. (B15) into the rhs of Eq. (B16), we find that Eq. (38) is recovered if

$$n_j = n_j^0 + n_j(\beta), \tag{B17}$$

provided n_j^0 is sufficiently small. The results of numerical calculations discussed below are obtained by solving the self-consistent set of RBCS + RQRPA equations and the one of MBCS + MQRPA equations, in which the quasiparticle occupation number n_j is approximated by Eq. (B17). Since n_j^0 in the calculations is found from Eq. (B8), which is in turn determined by the RQRPA amplitude $\mathcal{Y}_j^{(\nu)}$ (B12), the self-consistent solution can numerically verify the assumption of the smallness of n_j^0.

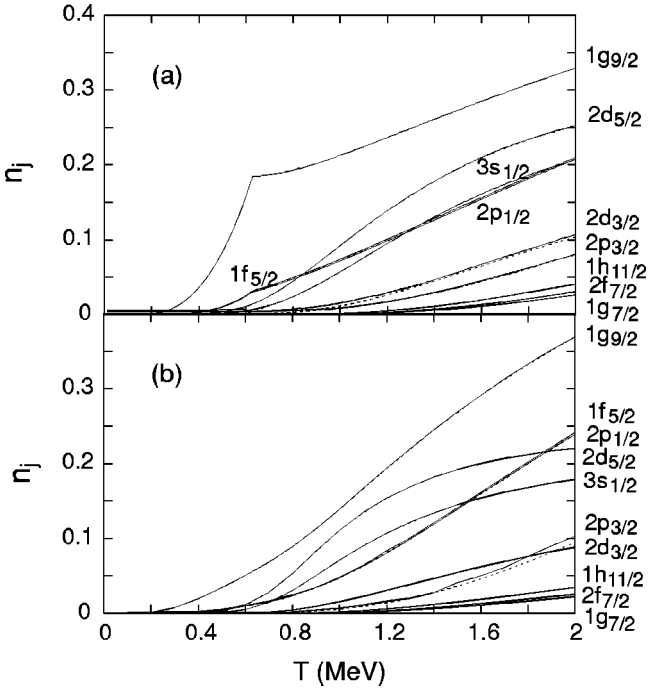

FIG. 7. Quasiparticle occupation numbers n_j corresponding to the levels in Table I for ^{74}Ni. The solid lines denote the $n_j = n_j^0 + n_j(\beta)$, while the dotted lines stand for only $n_j(\beta)$. Results obtained within the RBCS+RQRPA scheme are displayed in (a), while those obtained within the MBCS+MQRPA scheme are shown in (b).

3. Results of numerical calculations

Shown in Fig. 7 are quasiparticle occupation numbers n_j (B17) (solid lines) and $n_j(\beta)$ (29) (dotted lines), obtained within the RBCS+RQRPA scheme [Fig. 7(a)] and MBCS +MQRPA schemes [Fig. 7(b)] for ^{74}Ni. It is very clear on the figure that the solid and dotted lines practically coincide for all values of temperature T up to $T=2$ MeV. This feature is robust for all other nuclei considered in this paper. This means that n_j^0 is indeed negligible, and, therefore, approximation (30), which replaces n_j at $T\neq 0$ with the Fermi-Dirac distribution $n_j(\beta)$ of noninteracting quasiparticles, is indeed a very good approximation. This justifies all the calculations in the present paper, where $n_j(\beta)$ in Eq. (29) has been used instead of n_j.

It is worth mentioning that this work is restricted only to the pairing Hamiltonian (1) with monopole pairing interaction leading to the Cooper pairs. A more realistic model Hamiltonian, of course, contains also residual interaction of other multipolarities. Taking all the multipolarities into account, which is beyond the framework of the pairing problem considered here, enlarge the difference between n_j and $n_j(\beta)$. The self-consistent calculation including all multipolarities, e.g., up to $L=5$, is in fact a formidable task. Hence this could serve as an exciting challenge for future study.

[1] J. Bardeen, L. Cooper, and J. Schrieffer, Phys. Rev. C **108**, 1175 (1957).
[2] V.J. Emery and A.M. Sessler, Phys. Rev. **110**, 43 (1960).
[3] L. D. Landau and E. M. Lifshitz, *Course of Theoretical Physics*, Statistical Physics Vol. 5 (Nauka, Moscow, 1964), pp. 297 and 308.
[4] D.N. Zubarev, Sov. Phys. Usp. **3**, 320 (1960).
[5] A.L. Goodman, Nucl. Phys. **A352**, 30 (1981).
[6] L.G. Moretto, Nucl. Phys. **A182**, 641 (1972).
[7] A.L. Goodman, Phys. Rev. C **29**, 1887 (1984).
[8] N. Dinh Dang and N. Zuy Thang, J. Phys. G **14**, 1471 (1988).
[9] N.D. Dang, P. Ring, and R. Rossignoli, Phys. Rev. C **47**, 606 (1993).
[10] R. Rossignoli, P. Ring, and N.D. Dang, Phys. Lett. B **297**, 9 (1992).
[11] A. Volya, B.A. Brown, and V. Zelevinsky, Phys. Lett. B **509**, 37 (2001).
[12] V. Zelevinsky, B.A. Brown, N. Frazier, and M. Horoi, Phys. Rep. **276**, 85 (1996).
[13] N. Sandulescu, O. Civitarese, R.J. Liotta, and T. Vertse, Phys. Rev. C **55**, 1250 (1997).
[14] N. Sandulescu, O. Civitarese, and R.J. Liotta, Phys. Rev. C **61**, 044317 (2000).
[15] N. Dinh Dang and V. Zelevinsky, Phys. Rev. C **64**, 064319 (2001).
[16] J. Högaasen-Feldman, Nucl. Phys. **28**, 258 (1961).
[17] N. Dinh Dang, Z. Phys. A **335**, 253 (1990).
[18] K. Hagino and G.F. Bertsch, Nucl. Phys. **A679**, 163 (2000).
[19] F. Catara, N. Dinh Dang, and M. Sambataro, Nucl. Phys. **A579**, 1 (1994).
[20] Y. Takahashi and H. Umezawa, Collect. Phenom. **2**, 55 (1975); H. Umezawa, H. Matsumoto, and M. Tachiki, *Thermo Field Dynamics and Condensed States* (North-Holland, Amsterdam, 1982).
[21] N.N. Bogoliubov and S.V. Tyablikov, Sov. Phys. Dokl. **4**, 60 (1959).
[22] N.D. Dang and A. Arima, Phys. Rev. Lett. **80**, 4145 (1998); Nucl. Phys. **A636**, 427 (1998).
[23] P. Bonche, S. Levit, and D. Vautherin, Nucl. Phys. **A427**, 278 (1984).
[24] M. Brack and P. Quentin, Phys. Lett. **52B**, 159 (1974).
[25] M. Beiner, R. Lombard, and D. Mas, Nucl. Phys. **A249**, 1 (1975); J. Dobaczewski *et al.*, Phys. Rev. C **53**, 2809 (1996); M.V. Stoitsov, J. Dobaczewski, P. Ring, and S. Pittel, *ibid.* **61**, 034311 (2000).
[26] M. Grasso, N. Sandulescu, N. Van Giai, and R.J. Liotta, Phys. Rev. C **64**, 064321 (2001).
[27] H.J. Lipkin, Ann. Phys. (N.Y.) **31**, 525 (1960); Y. Nogami and I.J. Zucker, Nucl. Phys. **60**, 203 (1964); Y. Nogami, Phys. Lett. **15**, 335 (1965); J.F. Goodfellow and Y. Nogami, Can. J. Phys. **44**, 1321 (1966); H.C. Pradhan, Y. Nogami, and J. Law, Nucl. Phys. **A201**, 357 (1973).